Int J Solids Structures Vol 18 No 3, pp 181–197, 1982
Printed in Great Britain

0020-7683/82/030181-17$03.00/0
© 1982 Pergamon Press Ltd

A PLASTIC-FRACTURE MODEL FOR CONCRETE

S. S. HSIEH, E. C. TING and W. F. CHEN
School of Civil Engineering, Purdue University, West Lafayette, IN 47907, U S.A

(*Received* 20 *April* 1981; *in revised form* 3 *August* 1981)

Abstract—The paper summarizes recent efforts in formulating an elastic–plastic-fracture model for the finite-element analysis of concrete structures. Based on the geometrical considerations, a four-parameter fracture (or yielding) criterion was proposed which embraces some of the simpler existing models Isotropic elastic and anisotropic elastic behaviors were proposed for the initial loading and the post-failure behaviors A plastic model displaying mixed hardening was proposed to describe material behaviors between the initial yielding and the fracture failure Incremental stress–strain relationships were derived based on the associated flow rule and Ziegler's kinematic hardening rule Three different types of failure modes were considered A simple crushing coefficient was defined based on a dual criterion to identify the crushing type, the cracking type and the mixed type of failure Material parameters required for each element of the plastic-fracture model were determined. An important feature of the paper is that matrix formulations for all the constitutive equations were derived and are available for finite-element implementations

NOTATION

A, B, C, D experimentally determined material constants
$[b(\psi)], [b'(\psi)]$ abbreviated functions defined in eqns (24) and (25)
$c, \mathrm{d}\mu$ parameters in eqn (11) and eqn (12)
C_{ijkl} elastic stiffness tensor
$[C^{ep}], C_{ij}^{ep}$ tangent stiffness matrix of plastic concrete
$[\bar{C}]$ stiffness matrix of fractured concrete
E Young's modulus
$F(\bar{\sigma}_{ij}, \tau)$ loading function
f failure function
$f'_c, f'_t f'_{bc}, f'_{cc}$ ultimate strength of concrete under uniaxial compression, unaxial tension, biaxial equal compression and triaxial compression with confinement pressure f'_{pc}, respectively
f_c initial discontinuous strength of concrete under uniaxial compression
f'_{pc} confinement pressure for triaxial compression
G shear modulus
H work hardening modulus
$\bar{H}$ work hardening modulus associated with isotropic expansion
I_1 first stress invariant
$[I]$ identity matrix
J_2 second deviatroic stress invariant
K bulk modulus
M parameter of isotropic hardening effects
S_1 maximum principal deviatoric stress
S_{ij} deviatoric stress tensor
$[T_\sigma], [T_\epsilon]$ coordinate transformation matrices for stress and strain components
W abbreviated function in eqn (18)
α crushing coefficient
$\hat{\alpha}$ translation component for uniaxial compressive stress condition
α_{ij} translation components of the center of yielding surface
β reduction factor
β_i abbreviated functions in eqn (18)
δ_{ij} Kronecker delta
ϵ_i principal strains
ϵ_p' equivalent plastic strain due to isotropic hardening
$\mathrm{d}\epsilon_p$ equivalent plastic strain increment
$\mathrm{d}\epsilon_{ij}^e, \mathrm{d}\epsilon_{ij}^p, \mathrm{d}\epsilon_{ij}^{p'}, \mathrm{d}\epsilon_{ij}^{pk}$ elastic strain increment, plastic strain increment, isotropic hardening plastic strain increment, and kinematic hardening plastic strain increment, respectively
$\mathrm{d}\lambda$ positive scalar function in the normality condition
ν Poisson's ratio
(ρ, r, θ) Haigh–Westgarrd coordinate system
σ_i principal stresses
$\hat{\sigma}$ uniaxial compressive stress
$\bar{\sigma}_1$ maximum principal value of $\bar{\sigma}_{ij}$
$\bar{\sigma}_{ij}, \bar{S}_{ij}$ reduced stress and deviatoric stress components
σ_1, ϵ_1 maximum principal stress and strain
$\mathrm{d}\sigma_{ij}, \mathrm{d}\epsilon_{ij}, \{\mathrm{d}\sigma\}, \{\mathrm{d}\epsilon\}$ incremental stress and strain tensors
$\{\Delta\sigma\}, \{\Delta\epsilon\}$ incremental stress and strain matrices for the post-failure region
$\{\sigma_{ck}\}, \{\sigma_{ch}\}$ released stress matrices due to cracking and crushing, respectively
τ isotropic strain hardening rate function
ϕ abbreviated functions in eqn (18)
ψ angle that describes the crack plane direction

INTRODUCTION

With the rapid development of computer-aided design of structures, considerable research has been focused on the modeling of progressive failures exhibited in the concrete structures subjected to complex loading conditions. Different approaches for the mathematical modeling, such as material-nonlinear elasticity[1–3], rate-independent and rate-dependent plasticity theories[5–8] have been proposed in recent years A literature review including critiques of the various modeling techniques was given by Chen and Ting[9].

Concrete behaviors are exceedingly complicated. A constitutive model which embraces concrete characteristics for all types of loading and environmental conditions, and yet is sufficiently simple for present design applications, seems beyond reach. However, a reasonably complete constitutive model for short-time loadings should include some of the principal features of cracking behaviors: (i) The brittle cracking in tension, (ii) the ductile failure in compression, and (iii) the post-failure stress-redistribution due to local cracking. Focused on these three primary phenomena, we summarize in this paper our recent effort in formulating an elastic–plastic-fracture model for concrete structural analysis. The present consideration is limited to plain concrete behaviors subjected to tri-axial short-time loading conditions.

The model assumes a linear or nonlinear elastic stress–strain relationship until the combined state of stress reaches an initial yielding surface. The initial yielding criterion is assumed to have the same geometrical shape in the stress space as the failure criterion. A four-parameter failure criterion is also proposed to define the ultimate state of stress. Between the initial yielding state and the failure state, an incremental stress and strain relationship is assumed to define the plastic behaviors. The plastic relations are based on a mixed-hardening model and the classical associated flow rule. Fundamental concepts and the verification of the four-parameter failure criterion with experimental data are discussed. For the post-failure models, the concrete behaviors are defined by three different types of failure modes, namely, cracking, crushing, and a mixed mode. A crushing coefficient based on a dual criterion is proposed to identify each of the failure modes. Procedures have also been developed to handle the stress-redistribution for the fractured concrete. The procedures are tailored for the finite-element analysis of concrete structures. For the fractured concrete stress–strain relationship, an anisotropic elastic model is proposed.

Different stages of the proposed elastic–plastic-fracture model mentioned above can be illustrated schematically in a typical uniaxial stress–strain curve for plain concrete shown in Fig. 1.

A FOUR-PARAMETER FAILURE CRITERION

A four-parameter failure criterion is proposed to define the ultimate state of concrete behavior. The same form of formulation and the same proportionalities among the material parameters are also adopted to describe the initial yielding. This can be geometrically inter-

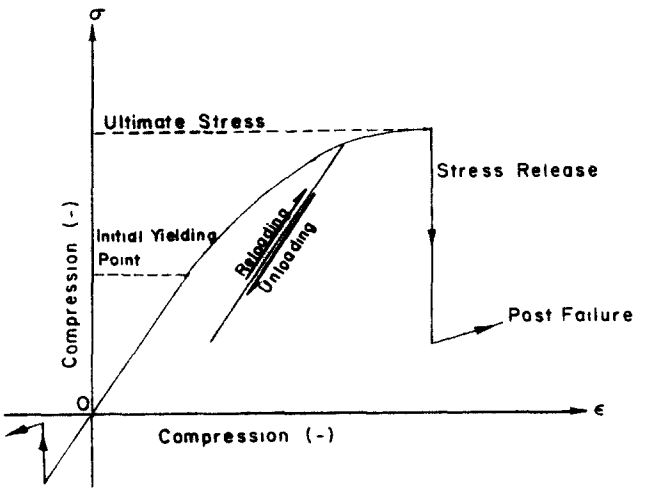

Fig 1 An idealized typical uniaxial stress–strain curve for plain concrete

preted as the initial yielding surface in the stress space has the same shape as the fracture surface. Only the limiting values are proportionally smaller. Concrete behaviors are assumed to be elastic for stresses within the initial yielding surface. For stresses falling between these two surfaces, concrete behaves plastically. Beyond the failure surface, an anisotropic elastic post-fracture behavior is assumed.

Characteristics of a failure surface

It is generally acceptable that the macroscopic fracture behavior can be assumed to be isotropic. This implies that a failure function can be written in terms of the principal stresses (σ_1, σ_2, σ_3) or in the Haigh–Westergärrd coordinate system [10] (the stress invariant space)

$$f(\rho, r, \theta) = 0 \tag{1}$$

where

$$\rho = \frac{1}{3} I_1,\ r = \sqrt{(2J_2)},$$

$$\theta = \cos^{-1} \frac{\sqrt{3}}{2} \frac{S_1}{\sqrt{2}},\ |\theta| \leq 60°,$$

S_1 = the maximum principal deviatoric stress

$$= \sigma_1 - \frac{1}{3} I_1 \text{ if } \sigma_1 > \sigma_2 > \sigma_3,$$

I_1 = the first stress invariant

$$= \sigma_1 + \sigma_2 + \sigma_3,$$

J_2 = the second deviatoric stress invariant

$$= \frac{1}{6}[(\sigma_1 - \sigma_2)^2 + (\sigma_2 - \sigma_3)^2 + (\sigma_3 - \sigma_1)^2].$$

A geometrical interpretation of the coordinate system is shown in Fig. 2. The explicit form of the failure function is defined by the experimental data. Uniaxial and biaxial tests of plain concrete are well-documented in the literature. To name a few, reports by Kupfer and Hilsdorf [11] and Tasuji *et al.* [12] nearly cover the full area of the biaxial stress section.

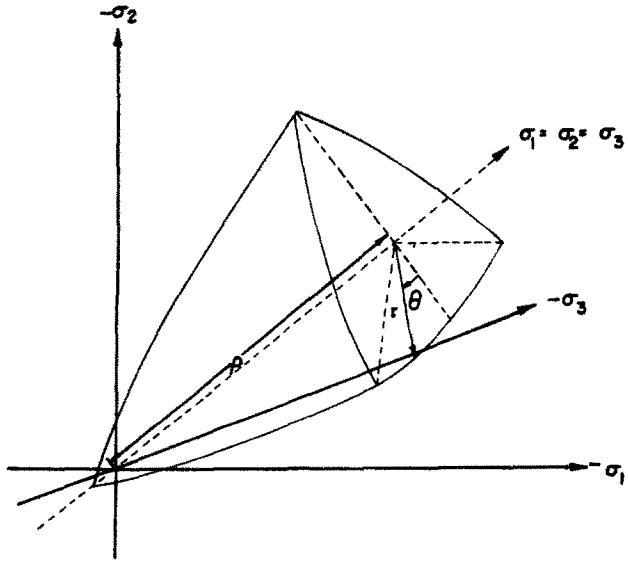

Fig. 2 General failure surface in principal stress space.

However, for the triaxial state, only the test data for limited ranges are available, and generally have wider scattering among different testing apparatus. Among them, we mention the results by Mills and Zimmerman[13] Launay and Gachon[14] and Gerstle *et al.*[15]. The aforementioned experimental data also forms the basis of the failure function proposed herein.

The available data clearly indicates that the failure surface plotted in the principal stress space, Fig. 2, should form a cone shape with smooth curved meridians and non-circular convex sections in the deviatoric stress plane. Since the hydrostatic pressure alone will not cause failure, the failure cone should have an open end in the negative hydrostatic axis. In addition, the intermediate principal stress should be accounted for. This indicates that the deviatoric cross-section of the failure cone approaches to a circular shape as the hydrostatic pressure increases. It proportionally shrinks into a triangular shape as the hydrostatic pressure decreases.

A four-parameter criterion

The present criterion is motivated by the geometrical requirements of the failure surface cross-section in the deviatoric plane mentioned above. Observe in Fig. 3 that for a constant value k, $r\cos\theta = k$ represents an equilateral triangle and $r = k$ is a circle on the deviatoric plane with $|\theta| \le 60°$. Hence, given two positive constants α and β with $\alpha + \beta = 1$, a combined equation $r(\alpha\cos\theta + \beta) = k$ yields a smooth function between $|\theta| \le 60°$ on the deviatoric plane and bounded by the two extremes of equilateral triangular and circular shapes ($\alpha = 0$ or $\beta = 0$). Recall the convex meridians shown in the experimental data. This indicates that for a constant value of θ, r should be a nonlinear function of ρ. Hence, ρ and r^2 terms are added and the resulting form is

$$f(\rho, r, \theta) = ar^2 + (\alpha\cos\theta + \beta)r + C\rho - 1 = 0. \tag{2}$$

Equation (2) may be written in terms of the stress invariants defined in eqn (1):

$$A\frac{J_2}{(f'_c)^2} + B\frac{\sqrt{J_2}}{f'_c} + C\frac{\sigma_1}{f'_c} + D\frac{I_1}{f'_c} - 1 = 0, \tag{3}$$

where the parameters are nondimensionalized by using the uniaxial compressive strength of concrete f'_c. In eqn (3), σ_1 is the maximum principal stress with a positive stress value representing a tensile stress. I_1 is the first stress invariant, and J_2 the second deviatoric stress invariant. It is interesting to note that although the basic form is originated by the geometrical consideration in the stress space, the resulting functional form appears to be a linear combination of three well-known failure criteria, namely, the von Mises, the Drucker–Prager, and the Rankine's criteria.

In some aspects, eqns (2) and (3) resemble the forms proposed recently by Ottosen[16], Hansson and Schimmelpfennig[17], Willam and Warnke[8], and Nagamatsu and Sato[18].

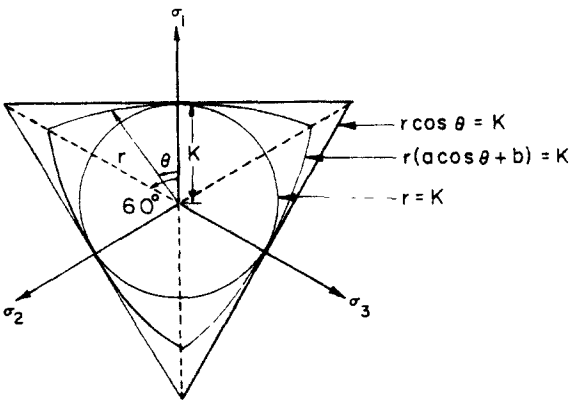

Fig 3 Geometry on the deviatoric plane

This is not surprising, since all the above forms are also based on the similar set of geometrical considerations. However, the present form appears to be simpler for the determination of material parameters and possesses some convenience in numerical calculation. Equations (2) and (3) also bear certain similarities to the forms suggested by Argyris *et al.*[19], Mills and Zimmerman[13] and Hannant and Frederick[20]. However, the present form has the advantage of satisfying the convexity requirements for all type of stresses. Verifications of the present failure criterion by plotting the function in the octahedral shear and normal stress plane, the biaxial stress plane, and the deviatoric stress plane have shown good agreement with the reported test data. For comparison, the material constants A, B, C, D in eqn (3) were evaluated based on four basic stress conditions: the simple tension ($\sigma_1 = f'_t, \sigma_2 = \sigma_3 = 0$), the simple compression (σ_1, $\sigma_2 = 0$, $\sigma_3 = -f'_c$), the biaxial compression ($\sigma_1 = 0$, $\sigma_2 = \sigma_3 = -f'_{bc}$), and the confined triaxial compression ($\sigma_1 = \sigma_2 = -f'_{pc}$, $\sigma_3 = -f'_{cc}$ with $f'_{cc} > f'_{pc}$). The stress values were assumed to be $f'_t = 0.1 f'_c$, $f'_{bc} = 1.15 f'_c$, $f'_{pc} = 0.8 f'_c$ and $f'_{cc} = 4.2 f'_c$. This gives $A = 2.0108$, $B = 0.9714$, $C = 9.1412$, and $D = 0.2312$. Figures 4–6 show the comparisons of the prediction and various reported data. We have also applied the failure criterion to study an elastic-fracture analysis of a concrete splitting test for the purpose of illustrating its tractability in numerical calculations[21].

Criterion for initial yielding

It is convenient to assume a criterion for initial yielding to have the same functional form as the failure criterion. In the present model, the material constants are also proposed to remain the same, except that the nondimensional constant, the compressive strength f'_c, is replaced by a different value $f_c = 0.3 \sim 0.6 f'_c$. The exact value of f_c can be taken from the uniaxial compressive stress–strain curve of the specific concrete used.

ELASTIC AND PLASTIC REGIONS

The initial yielding criterion and the failure criterion define the limits of the elastic region and the plastic region. Within the elastic region, concrete can be assumed to be an homogeneous, isotropic, linear elastic material from the macroscopic point of view. The constitutive relation is defined by a stress–strain relationship with two elastic constants, the modulus of elasticity E and Poisson's ratio ν, or alternatively, the bulk modulus K and shear modulus G. For finite-element applications, the matrix form of constitutive relations can be found in a standard textbook, e.g. Ref. [22]. For a state of stress beyond the initial yielding, irreversible

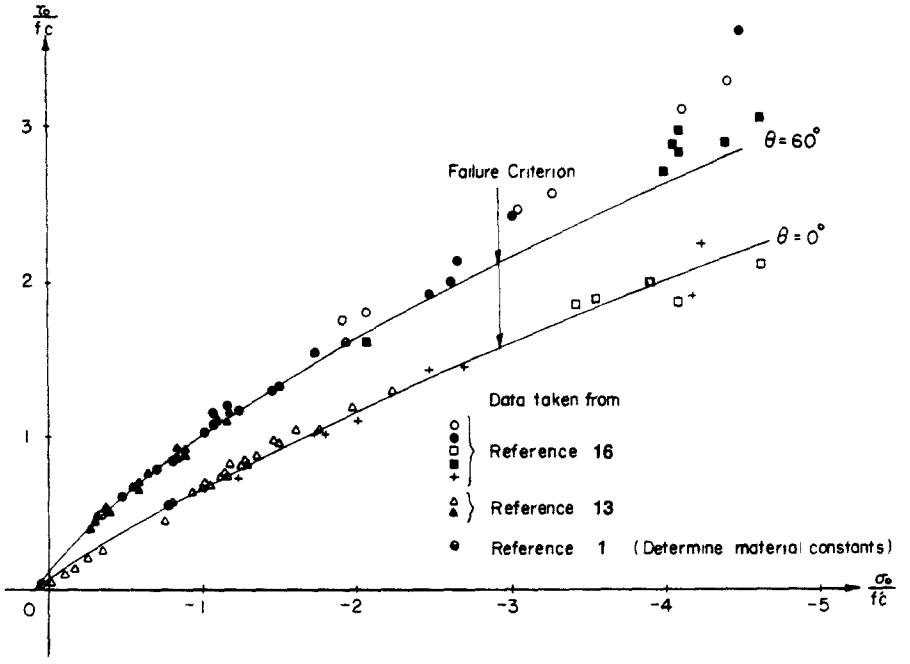

Fig 4 Failure criterion in octahedral shear and normal stress plane

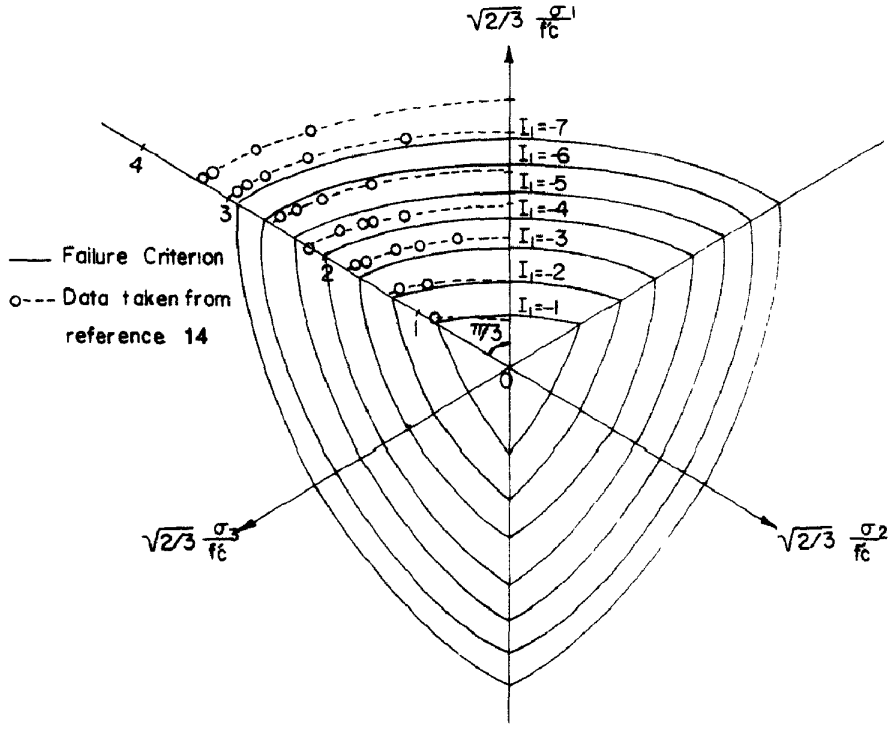

Fig. 5. Failure criterion in deviatoric stress plane

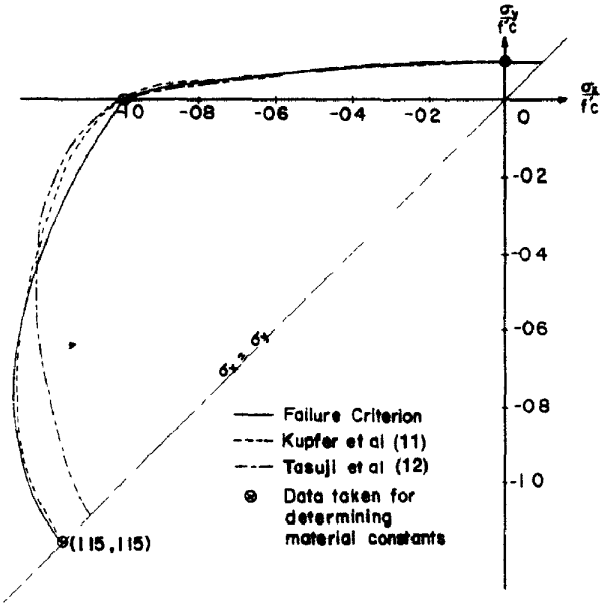

Fig. 6. Failure criterion in biaxial principal stress plane.

deformations become significant. It is convenient to follow the classical plasticity theory[10] to use an incremental form of stress–strain relationship. The total strain increment is taken to be the sum of the elastic increment and the plastic increment

$$d\epsilon_{ij} = d\epsilon^e_{ij} + d\epsilon^p_{ij}. \tag{4}$$

Adopting the flow rule with a plastic potential function F and

$$d\epsilon^p_{ij} = d\lambda \frac{\partial F}{\partial \sigma_{ij}}, \tag{5}$$

we may assume that the plastic potential coincides with the subsequent loading function which has a similar form as the initial yielding function or the failure function. In eqn (5), the associated flow rule, σ_{ij} is the total stress tensor and $d\lambda$ a positive parameter to be determined. To include concrete behaviors under the local unloading and the cyclic loading conditions, the kinematics of the loading surface is assumed to follow a mixed hardening model[23, 24]. The model allows the loading surface to translate and simultaneously to have isotropic expansion. The specific form of F is taken to be (Fig. 7)

$$F(\bar{\sigma}_{ij}, \tau) = A\frac{\bar{J}_2}{\tau(\epsilon_p')} + B\sqrt{\bar{J}_2} + C\bar{\sigma}_1 + D\bar{I}_1 + \tau(\epsilon_p') = 0, \tag{6}$$

where the tensor α_{ij} characterizes the translation of the center of the loading surface, $\tau(\epsilon_p')$ an isotropic hardening function, ϵ_p' the equivalent plastic strain due to isotropic hardening. A, B, C and D are material constants given in the failure criterion. The stress invariants are $\bar{I}_1 = \bar{\sigma}_{ii}$, $\bar{J}_2 = 1/2\,\bar{S}_{ij}\bar{S}_{ij}$ where $\bar{\sigma}_{ij} = \sigma_{ij} - \alpha_{ij}$, $\bar{S}_{ij} = S_{ij} - \alpha_{ij} + 1/3\delta_{ij}\alpha_{kk}$. S_{ij} is the deviatoric stress tensor and $\bar{\sigma}_1$ the maximum principal value of the stress tensor $\bar{\sigma}_{ij}$.

Using the condition of consistency, i.e. $dF = 0$, and noting that

$$\frac{\partial F}{\partial \bar{\sigma}_{ij}} = \frac{\partial F}{\partial \sigma_{ij}},$$

we have

$$\frac{\partial F}{\partial \sigma_{ij}}(d\sigma_{ij} - d\alpha_{ij}) + \frac{\partial F}{\partial \tau}d\tau = 0. \tag{7}$$

Equation (7) may be used to evaluate the flow rule parameter $d\lambda$. To do so, we consider the plastic strain increment. It is convenient to write

$$\begin{aligned} d\epsilon_{ij}^p &= d\epsilon_{ij}^{pl} + d\epsilon_{ij}^{pk} \\ &= M\,d\epsilon_{ij}^p + (1 - M)\,d\epsilon_{ij}^p, \end{aligned} \tag{8}$$

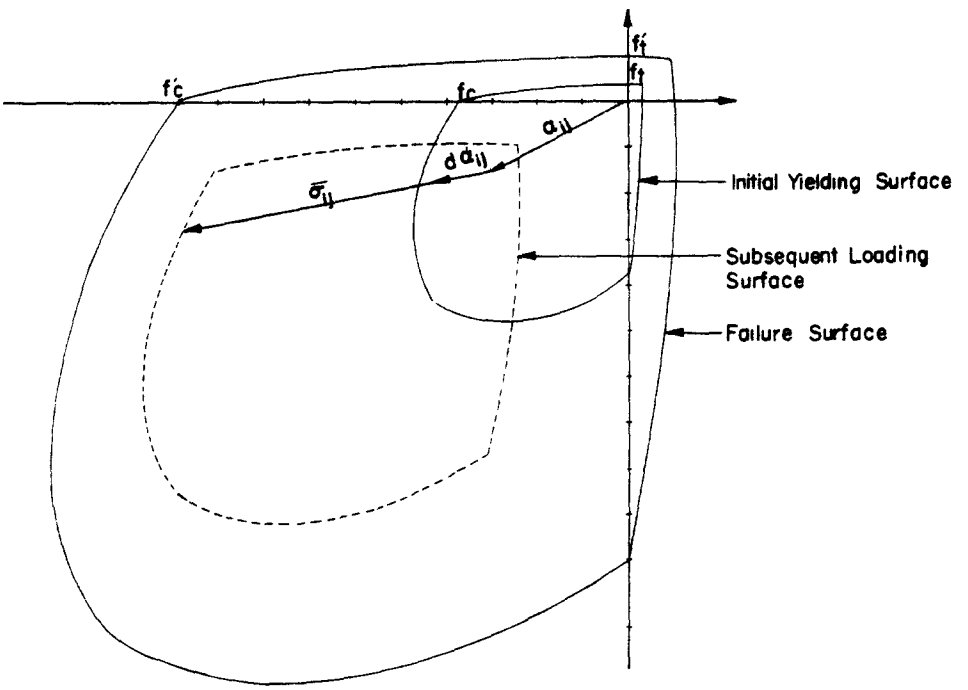

Fig. 7. Schematic of failure, initial yielding and subsequent loading surface.

and introduce a constant parameter M to define the isotropic hardening effect. The remaining plastic strain increment $d\epsilon_{ij}^{pk}$ is then due to the kinematic hardening. The strain increment $d\epsilon_{ij}^{pi}$ is related to the increment $d\tau$ of the isotropic hardening function. Define the equivalent plastic strain increment to be

$$d\epsilon_p = (d\epsilon_{ij}^p \, d\epsilon_{ij}^p)^{1/2}, \tag{9}$$

where the definition can be applied also to the components $d\epsilon_{ij}^{pi}$ and $d\epsilon_{ij}^{pk}$ which are denoted by $d\epsilon_p{}^i$ and $d\epsilon_p{}^k$, respectively. In view of the definition of the isotropic hardening function $\tau(\epsilon_p{}^i)$, we have

$$d\tau = \bar{H} \, d\epsilon_p{}^i = M\bar{H} \, d\epsilon_p, \tag{10}$$

where $\bar{H}$ is the slope of the $\tau - \epsilon_p{}^i$ curve.

To determine the tensor increment $d\alpha_{ij}$, Ziegler's kinematic hardening rule is assumed[25],

$$d\alpha_{ij} = d\mu\bar{\sigma}_{ij}. \tag{11}$$

The parameter $d\mu$ is further assumed to be a function of the kinematic strain increment in the form

$$d\mu = c \, d\epsilon_p{}^k = c(1 - M) \, d\epsilon_p. \tag{12}$$

Using the flow rule, eqn (5), to replace $d\epsilon_p$ by the corresponding stress components, $d\tau$ and $d\alpha_{ij}$ can be solved explicitly in terms of the unknown parameter $d\lambda$. Substituting the resulting forms into eqn (7) and noting that the elastic strain increment is governed by a linear elastic behavior,

$$d\sigma_{ij} = C_{ijkl} \, d\epsilon_{kl}^e \tag{13}$$

$$= C_{ijkl} \, d\epsilon_{kl} - d\lambda C_{ijkl} \frac{\partial F}{\partial \sigma_{kl}}, \tag{13}$$

where C_{ijkl} is the isotropic stiffness tensor whose components can be expressed in terms of elastic moduli. The parameter $d\lambda$ can be solved explicitly in term of the stress components. If $d\lambda$ is again substituted back into eqn (13), a total stress–strain incremental relationship for the plastic region is obtained:

$$d\sigma_{ij} = \left\{ C_{ijkl} - \frac{C_{ijmn} C_{klrs} C_{mnrs}}{C_{mnrs} C_{mnrs} + \left[c(1 - M) \dfrac{\partial F}{\partial \bar{\sigma}_{rs}} \bar{\sigma}_{rs} - \bar{H}M \dfrac{\partial F}{\partial \tau} \right] \sqrt{G_{mnmn}}} \right\} d\epsilon_{kl}, \tag{14}$$

where

$$G_{mnrs} = \frac{\partial F}{\partial \sigma_{mn}} \frac{\partial F}{\partial \sigma_{rs}} = \frac{\partial F}{\partial \bar{\sigma}_{mn}} \frac{\partial F}{\partial \bar{\sigma}_{rs}}.$$

Note that eqn (14) is based on the mixed hardening model. A weighting coefficient M is included to allow the freedom of selecting different proportions of isotropic and kinematic effects in the mixed model. M can also be a negative value, so that isotropic softening can be considered. The advantages of using the concept of mixed hardening have been demonstrated by Axelsson and Samuelsson[23] in describing the loading cycles of metals. They showed different degrees of Bauschinger effect can be considered. The mixed hardening gives much better curve-fitting results than either the isotropic or kinematic hardening model. In their consideration, M is arbitrarily set at 0.15 or 0.20.

Equation (14) also contains two material constants $\bar{H}$ and c. They can be related to the test results of a sample subjected to simple compressive loading. For the uniaxial compressive

stress condition, the only non-vanishing stress component is $\sigma_{33} = -\hat{\sigma}$, and according to Ziegler's hardening rule, the only corresponding non-vanishing component of α_{ij} is $\alpha_{33} = -\hat{\alpha}$. Hence, from the stress–plastic strain plot, we may evaluate the tangent modulus H, i.e

$$d\hat{\sigma} = H\, d\epsilon_p. \tag{15}$$

The degenerated form of the loading function given in eqn (6) becomes

$$\hat{\sigma} - \hat{\alpha} = \tau. \tag{16}$$

Using eqns (10)–(12) and eqn (16), we find

$$d\hat{\sigma} = M\bar{H}\, d\epsilon_p + c(1-M)\tau\, d\epsilon_p.$$

Or,

$$H = M\bar{H} + c(1-M)\tau.$$

Since M is arbitrary, this implies

$$\bar{H} = H \text{ and } c = \frac{H}{\tau}. \tag{17}$$

Finite-element implementation

To implement the incremental stress–strain relationship for finite-element analysis, it is convenient to write eqn (14) in an explicit matrix form. After carrying out the algebraic manipulation in substituting the loading function into eqn (14), we have

$$\{d\sigma\} = [C^{ep}]\{d\epsilon\}, \tag{18}$$

where

$$\{d\sigma\} = (d\sigma_x, d\sigma_y, d\sigma_z, d\tau_{yz}, d\tau_{xz}, d\tau_{xy})^T$$
$$\{d\epsilon\} = (d\epsilon_x, d\epsilon_y, d\epsilon_z, d\gamma_{yz}, d\gamma_{xz}, d\gamma_{xy})^T.$$

For $i = 1, 2, 3$,

$$C_{ii}^{ep} = \frac{E(1-\nu)}{(1+\nu)(1-2\nu)} - \frac{E^2}{W}\left(\frac{\beta_i}{1-2\nu} + \frac{\phi_i}{1+\nu}\right)^2.$$

For $i = 4, 5, 6$,

$$C_{ii}^{ep} = \frac{E}{2(1+\nu)} - \frac{E^2}{W}\left(\frac{\phi_i}{1+\nu}\right)^2.$$

For $i, j = 1, 2, 3$ and $i \neq j$,

$$C_{ij}^{ep} = \frac{E\nu}{(1+\nu)(1-2\nu)} - \frac{E^2}{W}\left(\frac{\beta_i}{1-2\nu} + \frac{\phi_i}{1+\nu}\right)\left(\frac{\beta_j}{1-2\nu} + \frac{\phi_j}{1+\nu}\right).$$

For $i = 1, 2, 3$ and $j = 4, 5, 6$

$$C_{ij}^{ep} = -\frac{E^2}{W}\left(\frac{\beta_i}{1-2\nu} + \frac{\phi_i}{1+\nu}\right)\frac{\phi_j}{1+\nu}.$$

For $i, j = 4, 5, 6$ and $i \neq j$,

$$C_{ij}^{ep} = -\frac{E^2}{W}\frac{\phi_i\phi_j}{(1+\nu)^2}$$

$$\phi_1 = \frac{\beta_2}{2\sqrt{\bar{J}_2}}\bar{S}_x + \beta_3[(\bar{S}_y\bar{S}_z - \bar{\tau}_{yz}^2 + \frac{1}{3}\bar{J}_2\Big],$$

$$\phi_4 = \frac{\beta_2}{\sqrt{\bar{J}_2}}\bar{\tau}_{yz} + 2\beta[\bar{\tau}_{xz}\bar{\tau}_{xy} - \bar{S}_x\bar{\tau}_{yz}].$$

ϕ_2 and ϕ_3 can be obtained by permutations of ϕ_1 for y and z. Similarly, ϕ_5 and ϕ_6 are obtained by permutations of ϕ_4.

$$W = \bar{H}M\left(\frac{A\bar{J}_2}{\tau^2} + 1\right)\sqrt{\left(2\beta_1^2 + \frac{2}{3}\beta_4\right)} + E\left(\frac{3\beta_1^2}{1-2\nu} + \frac{\beta_4}{1+\nu}\right)$$
$$+ c(1-M)[\bar{\sigma}_x(\beta_1+\phi_1) + \bar{\sigma}_y(\beta_1+\phi_2) + \bar{\sigma}_z(\beta_1+\phi_3)$$
$$+ \bar{\tau}_{yz}\phi_4 + \bar{\tau}_{xz}\phi_5 + \bar{\tau}_{xy}\phi_6]\sqrt{\left(2\beta_1^2 + \frac{2}{3}\beta_4\right)},$$

$$\beta_1 = \frac{1}{3}C + D,$$

$$\beta_2 = 2\sqrt{\bar{J}_2}\frac{A}{\tau} + B + \frac{2}{\sqrt{3}}\ C\left(\cos\theta - \frac{3\sqrt{3}}{2}\frac{\bar{J}_3}{\bar{J}_2^{3/2}}\frac{\sin\theta}{\sin 3\theta}\right),$$

$$\beta_3 = \frac{C}{\bar{J}_2}\frac{\sin\theta}{\sin 3\theta},$$

$$\beta_4 = \phi_1^2 + \phi_2^2 + \phi_3^2 + 2(\phi_4^2 + \phi_5^2 + \phi_6^2),$$

and

$$\theta = \frac{1}{3}\cos^{-1}\left[\frac{3\sqrt{3}}{2}\frac{\bar{J}}{\bar{J}_2^{3/2}}\right].$$

It should be noted that since the loading function becomes singular at $\bar{\sigma}_1 = \bar{\sigma}_2 > \bar{\sigma}_3$, or $\theta = 60°$, for this specific state of stress the limiting values of β_2 and β_3 should be implemented in the numerical calculations where

$$\beta_2 = 2\sqrt{\bar{J}_2}\frac{A}{\tau} + B + \frac{C}{\sqrt{3}},\ \beta_3 = 0.$$

A note of further interest is that since the failure criterion (and the loading function) is a generalization of several other theories of simpler form, it is particularly convenient from the program development point of view. For example, by suppressing material constants A and D and substituting appropriate material values for B and C, the computer program can be adopted for the Drucker–Prager's plasticity model[26]. By the choice of parameter $M = 0, 1$, or other values, we may select the hardening model to be kinematic, isotropic, or of the mixed type. Thus, the program developed based on the present model in fact embraces some simpler modeling techniques.

FAILURE MODE CRITERION

Concrete fails or fractures in extremely complex modes. Aggregate types, mixed design, and loading conditions among many other parameters all play important roles in the cause of failure It would be difficult to classify and define precisely the failure modes. However, in a general sense, the mode of failure may be categorized into three types, namely, the cracking, crushing and a mixture of cracking and crushing. Documented test results for tension–tension or

tension–compression biaxial conditions show the cause of fracture is primarily a brittle splitting in the plane normal to the maximum tensile strain direction (e.g. [12, 13, 27]). For the triaxial compression tests, depending on the magnitude of confinement pressure, it seems that all the three types of mode are possible. When the confinement pressure is much lower than the axial compression, rough crack surfaces can be formed in the direction normal to the maximum tensile strain, possibly due to the connection of numerous microcracks. For nearly uniform hydrostatic condition, crushing failure is more common, possibly due to the rupture of mortar in the concrete.

Crushing coefficient

In view of the failure modes due to various types of loading conditions, a crushing coefficient α is proposed to identify the mode being either a pure cracking, a pure crushing, or a mixture of the above. The coefficient can also be used to estimate the proportions of cracking effect or the crushing effect in a mixed type failure. This is particularly convenient when the post-failure behaviors of the fractured concrete are considered.

The concept of crushing coefficient is based on the consideration of a dual criterion in defining the pure cracking zone and the pure crushing zone in the overall spectrum of failure mode. Specifically, the pure cracking zone is assumed to satisfy the maximum tensile stress condition

$$\sigma_1 > 0.$$

Written in terms of the stress invariants, we have

$$J_2 \cos\theta + \frac{1}{2\sqrt{3}} I_1 > 0, \quad |\theta| \leq 60^\circ \tag{19}$$

It may be shown that the upper limit of the pure cracking condition satisfies the uniaxial and the biaxial compression failure test data, see Fig. 8. For the pure crushing zone, it seems reasonable to assume that all three principal strain components are all compressive strains, so that the crack mechanism can not be developed in the light that no tensile strain could appear in any direction. This implies that the maximum principal strain is non-positive

$$\epsilon_1 < 0.$$

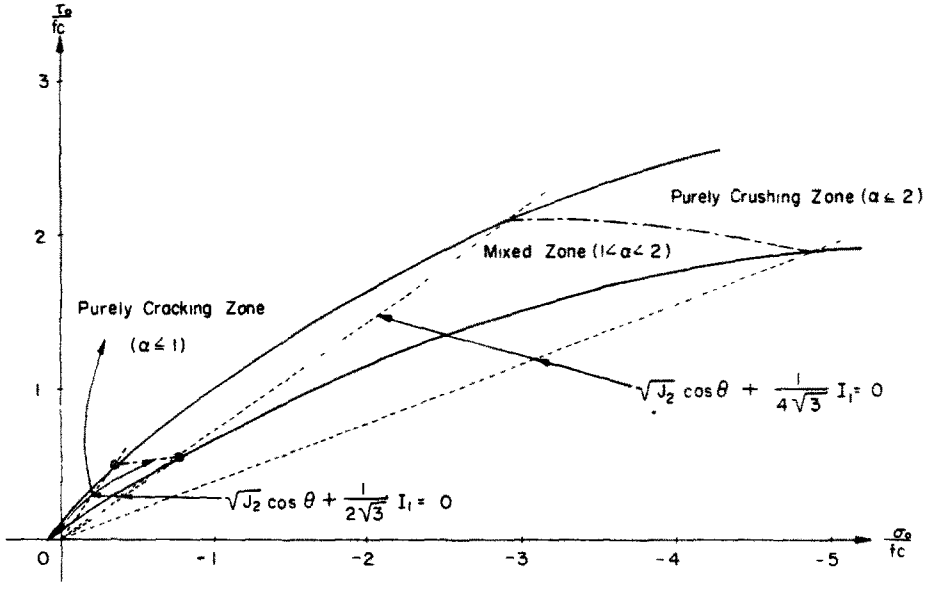

Fig 8 Failure zones in octahedral shear and normal stress plane

Using the Hooke's law, the same condition becomes

$$\sigma_1 - \nu(\sigma_2 + \sigma_3) < 0 \quad \text{with} \quad \sigma_1 > \sigma_2 > \sigma_3.$$

Rewrite the inequality in terms of the stress invariants, it becomes

$$\sqrt{J_2}\cos\theta + \frac{(1-2\nu)}{2\sqrt{3}(1+\nu)} I_1 < 0, \quad |\theta| \leq 60°. \tag{20}$$

Combining eqns (19) and (20) a crushing coefficient α is defined as

$$\alpha = -\frac{I_1}{2\sqrt{3}\sqrt{J_2}\cos\theta}, \quad |\theta| \leq 60°. \tag{21}$$

The failure modes are then identified as

(i) Pure cracking, $\alpha < 1$,

(ii) Pure crushing, $\alpha > \dfrac{(1+\nu)}{(1-2\nu)}$, (22)

(iii) Mixed mode, $1 \leq \alpha \leq \dfrac{(1+\nu)}{(1-2\nu)}$.

If Poisson's ratio is taken to be $\nu = 0.2$, we have $\alpha = 1.0$ and 2.0 as the boundary values separating the three different failure zones.

Note that in obtaining the simple crushing coefficient α Hooke's law of elasticity was employed to obtain the stress criterion. Strictly speaking, this is inconsistent in an elastic-plastic-fracture model; Hooke's law may not apply immediately before crushing. However, judging by the complex nature of concrete failure and the simplicity in the application of the crushing coefficient, the elasticity assumption may represent an acceptable approximation. For more accurate descriptions, the original dual criterion, i.e. $\sigma_1 > 0$ and $\epsilon_1 < 0$, may also be used.

POST-FAILURE BEHAVIOR OF FRACTURED CONCRETE

To complete the constitutive model, we also need to define the post-failure behaviors for each of the failure modes identified by the crushing coefficient. For the pure crushing zone, the crushed concrete can be viewed to behave like a grannular material under the confinement of neighboring materials. Material stiffness in compression or shear, although reduced, should still exist. However, for simplicity, we may neglect the residual stiffness and the residual strength of a crushed concrete element in the analysis. Thus, the post-failure behavior becomes perfectly deformable. For a concrete element subjected to pure cracking, the post-failure behavior is assumed to be anisotropic elastic that the element have lost its rigidity in the cracked planes, see Fig. 9. An extensive discussion of the kinematics of a cracked concrete element was reported by Chen and Suzuki[28]. Within the mixed failure zone, the value of the crushing coefficient is between 1.0 and 2.0 for $\nu = 0.2$, for example. If the crushing coefficient is adopted as a measure of the degree of crushing in this partially cracking and partially crushing concrete element, then we may view that the post-failure behavior is also a linear interpolation of the perfectly deformable behavior and the anisotropic elastic behavior. Hence, it is proposed that the concrete element will lose its rigidity in the cracked plane according to the maximum tensile strain direction and the anisotropic stiffness of the fractured element will also be proportionally reduced according to the magnitude of α. Note that for $\nu = 0.2$, mixed failure lies between $\alpha = 1.0$ and $\alpha = 2.0$. Thus, the values of α behind the decimal point represents the percentages of crushing and also the percentages of stiffness reduction.

Finite-element implementation

To formulate the anisotropic elastic behaviors in matrix form for finite-element application,

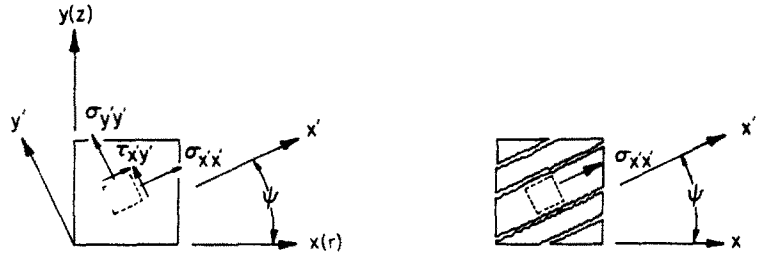

(a) Stress Distribution Just Before Cracks Are Formed

(b) Stress Distribution Just After Cracks Are Formed

Fig 9 Pattern of cracks and stress distribution in a cracked concrete

we define the pre-failure principal axes be (x', y', z') with x' denoting the maximum tensile strain direction. Then, the incremental stress–strain relation for the post-failure behavior has the form

$$\{\Delta\sigma\} = [T_\sigma]^T[\bar{C}][T_\epsilon]\{d\epsilon\} - \{\sigma_{ck}\} - \{\sigma_{ch}\}, \tag{23}$$

in which

$$\{\Delta\sigma\} = \{\Delta\sigma_x, \Delta\sigma_y, \Delta\sigma_z, \Delta\tau_{yz}, \Delta\tau_{xz}, \Delta\tau_{xy}\}^T,$$
$$\{\Delta\epsilon\} = \{\Delta\epsilon_x, \Delta\epsilon_y, \Delta\epsilon_z, \Delta\gamma_{yz}, \Delta\gamma_{xz}, \Delta\gamma_{xy}\}^T,$$
$$\{\sigma_{ck}\} = [T_\sigma]^T\{\sigma'_x, 0, 0, 0, \tau'_{xz}, \tau'_{xy}\}^T,$$
$$\{\sigma_{ch}\} = (\beta - 1)[T_\sigma]^T\{0, \sigma'_y, \sigma'_z, \tau'_{yz}, 0, 0\}^T.$$

$\{\sigma_{ck}\}$ is the released stress components due to cracking and $\{\sigma_{ch}\}$ is that due to crushing. $[T_\sigma]$ and $[T_\epsilon]$ are the transformation matrices for stress and strain components between the principal coordinates and the original reference frame. β is a reduction factor related to the crushing coefficient α. For $\alpha < 1$, $\beta = 1$; $\alpha > 2$, $\beta = 2$; and $1 \le \alpha \le 2$, $\beta = \alpha$. $[\bar{C}]$ is a stiffness matrix with components

$$\bar{C}_{22} = \bar{C}_{33} = (2-\beta)E(1-\nu)/(1+\nu)(1-2\nu),$$
$$\bar{C}_{23} = \bar{C}_{32} = (2-\beta)E\nu/(1+\nu)(1-2\nu),$$
$$\bar{C}_{44} = (2-\beta)E/2(1+\nu),$$

and all other components vanishes.

It is expedient to list the matrix equations for some special cases:

(a) *The axisymmetrical problem.* Written in polar coordinates, we have

$$\begin{Bmatrix} \Delta\sigma_r \\ \Delta\sigma_z \\ \Delta\tau_{rz} \\ \Delta\sigma_\theta \end{Bmatrix} = \frac{(2-\beta)E}{1-\nu^2} \left\langle \begin{array}{c|c} \{b(\psi)\}\{b(\psi)\}^T & \nu\{b(\psi)\} \\ \hline \nu\{b(\psi)\}^T & 1 \end{array} \right\rangle \begin{Bmatrix} \Delta\epsilon_r \\ \Delta\epsilon_z \\ \Delta\gamma_{rz} \\ \Delta\epsilon_\theta \end{Bmatrix} - \left\langle \begin{array}{c|c} [I] - (2-\beta)\{b(\psi)\}\{b'(\psi)\}^T & 0 \\ \hline 0 & \beta - 1 \end{array} \right\rangle \begin{Bmatrix} \sigma_r \\ \sigma_z \\ \tau_{rz} \\ \sigma_\theta \end{Bmatrix} \tag{24}$$

(b) *The plane strain problem.*

$$\begin{Bmatrix} \Delta\sigma_x \\ \Delta\sigma_y \\ \Delta\tau_{xy} \end{Bmatrix} = \frac{(2-\beta)E}{1-\nu^2} \left(\{b(\psi)\}\{b(\psi)\}^T \right) \begin{Bmatrix} \Delta\epsilon_x \\ \Delta\epsilon_y \\ \Delta\gamma_{xy} \end{Bmatrix} - ([I] - (2-\beta)\{b(\psi)\}\{b'(\psi)\}^T) \begin{Bmatrix} \sigma_x \\ \sigma_y \\ \tau_{xy} \end{Bmatrix} \tag{25}$$

The abbreviated functions are

$$\{b(\psi)\} = \begin{Bmatrix} \cos^2\psi \\ \sin^2\psi \\ \sin\psi\cos\psi \end{Bmatrix} \text{ and } \{b'(\psi)\} = \begin{Bmatrix} \cos^2\psi \\ \sin^2\psi \\ 2\sin\psi\cos\psi \end{Bmatrix},$$

where ψ is the direction of the cracked plane, see Fig. 9, $[I]$ is the identity matrix.

(c) *The plane stress problem.* Special attention should be given to the plane stress condition. For tension–tension and tension–compression conditions, the maximum tensile stress is in the plane, and the concrete always fails in the cracking mode. However, for the compression–compression case, normal stress $\sigma_1 = 0$ represents the maximum stress. This indicates that the crushing parameter $\alpha = 1.0$ for all stresses. Hence, for plane stress condition the mixed zone and crushing zone are collapsed into a singular point. Physically, it can be interpreted that based on the zero-thickness assumption of plane stress, the element thickness simply does not permit cracks to generate, and pure crushing would result due to the simultaneous compressions in the plane. The corresponding matrix formulations are: for tension–tension and tension–compression cases,

$$\begin{Bmatrix} \Delta\sigma_x \\ \Delta\sigma_y \\ \Delta\tau_{xy} \end{Bmatrix} = [E\{b(\psi)\}\{b(\psi)\}^T] \begin{Bmatrix} \Delta\epsilon_x \\ \Delta\epsilon_y \\ \Delta\gamma_{xy} \end{Bmatrix} - ([I] - \{b(\psi)\}\{b'(\psi)\}^T) \begin{Bmatrix} \sigma_x \\ \sigma_y \\ \tau_{xy} \end{Bmatrix},$$

and for compression–compression case,

$$\begin{Bmatrix} \Delta\sigma_x \\ \Delta\sigma_y \\ \Delta\tau_{xy} \end{Bmatrix} = [\mathbf{0}] \begin{Bmatrix} \Delta\epsilon_x \\ \Delta\epsilon_y \\ \Delta\gamma_{xy} \end{Bmatrix} - \begin{Bmatrix} \sigma_x \\ \sigma_y \\ \tau_{xy} \end{Bmatrix}.$$

APPLICATION FOR OTHER MATERIALS

The present model is proposed for concrete materials. However, the model can also be extended to represent properties of other engineering materials of similar nature. As mentioned previously, by inserting appropriate material constants (see Table 1) the model can be degenerated to simpler forms, such as the von Mises criterion which has been used for metals. It can also be reduced to the Drucker–Prager criterion which has been used as a simplified version for the Mohr–Coulomb model for rocks and soils. The proposed four-parameter failure criterion and the associated constitutive equations are thus the generalization of some models used for a wide variety of materials. Due to the flexibility of having four material constants, material properties can be simulated more accurately. For example, the Drucker–Prager yield

Table 1 Material constants matched with other criteria

Four-Parameter Model	A	B	C	D
von Mises ($\sqrt{J_2} = K$)	0	$\frac{1}{K}$	0	0
Drucker-Prager ($I_1 + \sqrt{J_2} = K$)	0	$\frac{1}{K}$	0	$\frac{\alpha}{K}$
Coulomb ($\tau + \sigma\tan\phi - c = 0$)	0	$\frac{\sqrt{3}(1-\sin\phi)}{2c\cos\phi}$	$\frac{1}{c}\tan\phi$	0

function, depicted in the three dimensional principal stress space, can be represented by a cone shape with the circular base located on the deviatoric stress plane, while the Coulomb criterion is a pyramid shape with an irregular hexagonal base. Thus discrepancies are expected when the Drucker–Prager model is used to simulate the behaviors of a typical Coulomb-type material such as soils. Efforts have been made to minimize the discrepancies by relating the Drucker–Prager constants α and K to the Coulomb coefficients c and ϕ by using various matching approaches. However, successful matchings are limited to certain special cases. Using the four-parameter model proposed in the study the material constants A, B, C, D can be used to match Coulomb's material properties ϕ and c as shown in Table 1. With two additional constants they seem to match very well on the deviatoric plane. The difference is less than 4% (see Fig. 10). Plotted both criteria on the biaxial stress plane, without further adjustment in the material constants, the maximum difference is found to be less than 15% in the compression–compression region and 4% in the tension–compression and the tension–tension regions as shown in Fig. 11.

SUMMARY AND CONCLUSIONS

A plastic-fracture constitutive model for concrete structural analysis has been developed, with the primary objective being that the material model has the capability of describing the essential features of concrete behaviors, and is yet sufficiently simple for which the model can easily be implemented for finite-element analysis. Based on the geometrical considerations in the stress space, a four-parameter failure (yielding) criterion is proposed. Parameter determination for the criterion has shown to be simple. In addition, the criterion proves to be a linear combination of three simple models, namely, von Mises, Drucker–Prager and Rankine models. Hence, a plastic-fracture theory based on the present failure (yielding) criterion in fact embraces some simpler theories. This is particularly tractable in the program development and in the selection of modeling techniques often required in the material characterization. Resting on the similar consideration, a plastic model displaying mixed hardening effect has been proposed. With the selection of a constant parameter, the hardening rule has the choice among the isotropic type, the kinematic type, and the mixed type.

To identify the failure mode, a simple crushing coefficient based on a dual criterion is proposed to subdivide the spectrum of failure into the crushing type, the cracking and a mixture of cracking and crushing. For each type of the failure modes, the post-failure anisotropic elastic behavior has been defined. The crushing coefficient is also used to estimate the amount of crushing in the mixed mode of failure, and to determine the loss of material rigidity after fracture.

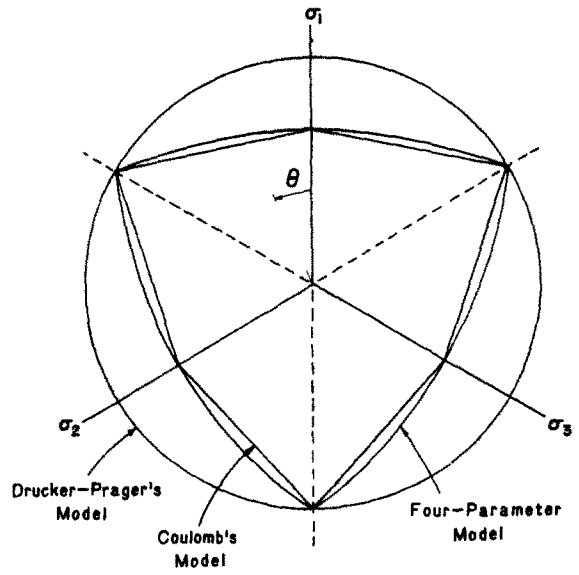

Fig 10 Mohr-Coulomb model, Drucker-Prager model and the four-parameter model in deviatoric stress plane.

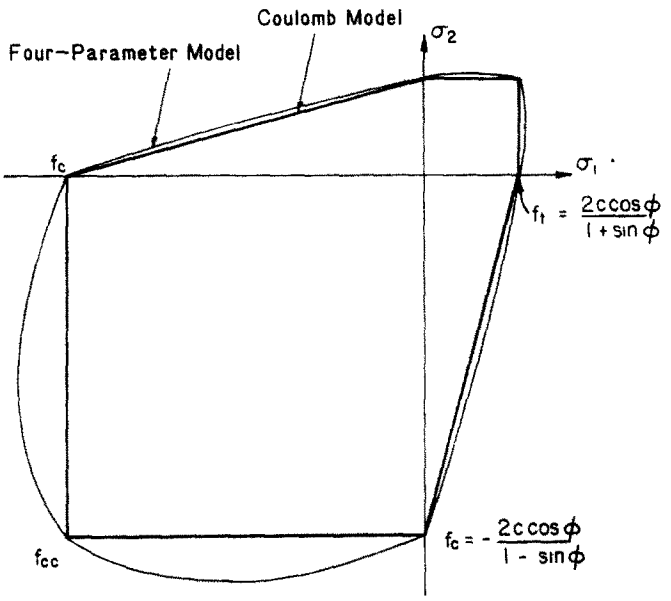

Fig. 11 Comparison of Mohr–Coulomb model and the four-parameter model in biaxial stress plane.

Since one of the considerations in the development is that the material model developed should be convenient for numerical calculations, matrix equations for the constitutive relationships at all stages of the loading and unloading process discussed in the above have been explicitly formulated. This includes the consideration of adopting a stress-redistribution process commonly used in finite-element analysis to handle the progressive failures.

In conclusion, we wish to emphasize the generality and versatility of the present plastic-fracture model, the simplicity in using the crushing coefficient to handle various types of failure mode, and the tractability in implementing the model for concrete structural analysis.

REFERENCES

1 L. Cedolin, Y. R J Crutzen and S. D Poli, Triaxial stress–strain relationship for concrete *J Engng Mech. Div* ASCE **103**(EM3), 243–439, Proc Paper 12969 (June 1977)
2 T C Y Liu, A H Nilson and F O Slate, Biaxial stress–strain relations for concrete, *J Struct. Div* ASCE, **98**(ST5), 1025–1034 Proc Paper 8905 (May 1972)
3 R Palaniswamy and S. P. Shah, Fracture and stress–strain relationship of concrete under triaxial compression *J Struct Div.* ASCE, **100**(ST5), 901–916 Proc Paper 10547 (May 1974)
4 Z P Bažant and P D Bhat, Endochronic theory of inelasticity and failure of concrete. *J Engng Mech. Div.* ASCE **102**(EM4), 701–722 Proc Paper 12360 (Aug. 1976)
5 Z P Bažant and C L Shieh, Endochronic model for nonlinear triaxial behavior of concrete *Nuclear Engng Design* **47**, 305–315 (1978)
6 A C T Chen and W F Chen, Constitutive relations for concrete *J Engng Mech. Div.* ASCE **101**(EM4), 465–481 Proc Paper 11529 (Aug 1975)
7 A C. T Chen and W. F Chen, Constitutive equations and punch-indentation of concrete *J Engng Mech. Div* ASCE, **101**(EM6), 889–906. Proc Paper 11809 (Dec 1975)
8 K J Willam and E P Warnke, Constitutive model for the triaxial behavior of concrete. International Association of Bridge and Structural Engineers Seminar on Concrete Structures Subjected to Triaxial Stresses, Paper III-I, Bergamo, Italy, 17–19 May, 1974
9 W. F. Chen and E C. Ting, Constitutive models for concrete structures *J Engng Mech. Div* ASCE **106**(EM1), 1–19. Proc Paper 15177 (Feb 1980)
10 A Mendelson, *Plasticity Theory and Applications* McMillan, New York (1968)
11. H Kupfer and H K. Hilsdorf, Behavior of concrete under biaxial stresses *ACI J* **66**(8), 656–666 (Aug. 1969).
12. M. E Tasuji, F O Slate and A H Nilson, Stress–strain response and fracture of concrete in biaxial loading *ACI J* **75**(7), 306–312 (July 1978)
13 L. L Mills and R M. Zimmerman, Compressive strength of plain concrete under multiaxial loading conditions *ACI J.* **69**(10), 802–807 (Oct 1970)
14 P. Launay and H. Gachon, Strain and ultimate strength of concrete under triaxial stress *Special Publ.*, SP-34, ACI 1, 269–282 (1970)
15 K H. Gerstle *et al*, Strength of concrete under multiaxial stress states *Special Publ* SP55-5, 103–131 ACI, Douglus McHenry International Symposium on Concrete and Concrete Structures (1978)
16 N S Ottosen, A failure criterion for concrete *J Engng Mech Div* ASCE **103**(EM4), 527–536 Proc Paper 13111 (Aug 1977)

17 V. Hansson and K Schimmelpfennig, Concrete strength in multiaxial stress states *Special Publ* SP-34, ACI, 1, 295–309 (1970).
18. S. Nagamatsu and A. Sato, Study on fracture criterion of concrete under combined stress, (Part I–III). *Trans AIJ*, No. 246, 247, 254, 7–15, 1–10, 11–20 (Aug., Sept 1976, April 1977)
19. J. H. Argyris, G. Faust, J. Szimmat, E. P. Warnke and K. J Willam, Recent developments in the finite element analysis of prestressed concrete reactor vessels. *Nuclear Engng Design* **28**, 42–75 (1974)
20. D. J Hannant and C O. Frederick, Failure criteria for concrete in compression, *Magazine of Concrete Res* **20**(64), 137–144 (Sept. 1968)
21. S S. Hsieh, E. C. Ting and W. F Chen, An elastic-fracture model for concrete *3rd ASCE/EMD Specialty Conf.*, Austin, Texas, 437–441 17–19 Sept. 1979.
22 O. C. Zienkiewicz, *The Finite Element Method in Engineering Science*, McGraw-Hill, London (1971).
23 K. Axelsson and A. Samuelsson, Finite element analysis of elastic–plastic materials displaying mixed hardening. *Int. J. Num. Meth. Engng* **14**, 211–225 (1979).
24. H. A. Balmer and J. St Doltsinis, Extensions to the elastoplastic analysis with the ASKA program system *Comput. Meth. in Appl. Mech. Engng* **13**, 363–401 (1978)
25. H. Ziegler, A modification of Prager's hardening rule *Quart Appl. Mathematics* **17**, 55–65 (1959).
26. D. C. Drucker and W. Prager, Soil mechanics and plasticity analysis of limit design, *Quart. Appl. Mathematics* **10**(2), 157–165 (1952)
27. J. N Carino and F. O Slate, Limiting tensile strain criterion for failure of concrete, *ACI J* **73**(3), 160–165 (1976).
28 W F Chen and H Suzuki, Constitutive models for concrete, ASCE Annual Convention and Exposition, Chicago, Illinois, October 16–20, 1978, *Preprint* 3431, 51–79